Journal of Alloys and Compounds 505 (2010) 516–522

Contents lists available at ScienceDirect

Journal of Alloys and Compounds

journal homepage: www.elsevier.com/locate/jallcom

Review

Laser melted ZrO_2–Y_2O_3 thermal barrier obtained by plasma spraying method

Krystyna Kobylańska Szkaradek*

Silesian University of Technology, 40-019 Katowice, Krasinskiego 8, Poland

ARTICLE INFO

Article history:
Received 9 July 2009
Accepted 18 June 2010
Available online 1 July 2010

Keywords:
Thermal barrier coatings (TBC)
Air plasma spraying (APS)
Laser treatment
Thermal conductivity

ABSTRACT

The aim of the paper is to determine the influence of laser melting upon the selected physical properties of ZrO_2–Y_2O_3 ceramic coatings deposited by APS method on super-alloys which function as TBC. Laser melting which helps to eliminate pores and other structural defects of coatings deposited by plasma spraying method should contribute to the improvement of their density and durability as thermal barriers. In order to prove the assumptions made in the paper, coatings featuring varied porosity and deposited upon the nickel base super-alloys surface with the initially sprayed NiCrAlY bond coat have been subjected to laser melting and then their structure, thermal conductivity and thermal life prediction in the conditions of cyclic temperature changes from 20 to 1200 °C have been examined. It has been revealed that the coatings featuring low porosity where laser melted on part of their thickness and heated up to about 700 °C, demonstrated the highest thermal life prediction under the above conditions mentioned and at slightly lower thermal conductivity. It has been found that homogenization of chemical composition of coatings occurs during laser melting leading to the reduction of ZrO_2–Y_2O_3 phase with monoclinic lattice participation as well as to the reduction of structural stresses which accompany this phase transformation during heating and cooling process. The worked out conditions of laser melting might be used in the process of creation of ZrO_2–Y_2O_3 coats which feature high working durability upon super-alloy elements.

Contents

1. Introduction

Oxide ceramic materials feature high melting temperature, relatively low density and low thermal conductivity as well as considerable corrosion resistance to chemically active media in high temperatures. They feature high compressive and bend strength though their brittle character restricts their application as constructional materials. Ceramic coatings, however, seem more effective as thermal barriers TBC deposited upon surfaces of super-alloy surfaces, operating under load in high temperatures. Low thermal conductivity of ceramic materials in comparison with metals determine the fact that the high thermal gradient formed in relatively thin coating significantly reduces the working temperature of the metal substrate in the metal element as compared to the temperature of thermodynamic factor, i.e. gas or wastes. It is then possible to increase both the operating temperature and thermal efficiency especially in case of aeronautical gas turbines and stationary turbines. The above seems important as it is quite problematical how to increase creep resistance of metal alloys. The maximum operating temperature of monocrystalline gas turbine blades produced nowadays from nickel base alloys is close to 1100 °C, and the increase creep

* Tel.: +48 032 6034 153.
E-mail address: Krystyna.Kobylanska-Szkaradek@polsl.pl.

0925-8388/$ – see front matter © 2010 Elsevier B.V. All rights reserved.
doi:10.1016/j.jallcom.2010.06.114

Table 1
Chemical composition, granularity and morphology of powders [12].

Powder mixture	Contents (wt.%)	Granularity (μm)	Powder morphology
Amdry 961	76.5%Ni + 17%Cr + 6%Al + 0.5%Y	105	Spherical gas sprayed
Metco 204B–NS	92%ZrO_2 + 8%Y_2O_3	74	Spherical HOSP[a]of high purity

[a] Hole Structure Powder-porous.

resistance of metal alloys. The maximum operating temperature of monocrystalline gas turbine blades produced nowadays from nickel base alloys is close to 1100 °C, and the application of ceramic thermal barriers helps increase it by about 100 °C [1,2].

ZrO_2 plus 8 wt.% Y_2O_3 which stabilizes the modification of this ceramic material with a cubic lattice up to the melting temperature over 2700 °C generates considerable interest [3,4]. Ensuring greater structural stability makes it possible to avoid stresses which appear between metal substrate and ceramic coating. The stresses are closely related to phase transformation of the structure during heating and cooling processes. Various interatomic bonds of ceramic material and alloys determine relatively weak bonds between these materials. Moreover, much lower thermal expansion of the ceramic material as compared with the substrate generates thermal stresses in the ceramic coating which subsequently reduces their durability. In order to improve bonds between these materials, ceramic coatings are deposited upon metal substrate with considerable surface roughness, usually after initial deposition of e.g. NiCrAlY alloy coat featuring hot corrosion resistance and mean value of thermal expansion coefficient related to right expansion for ceramic material and substrate. This increases adhesion of coatings to metal substrate and decreases thermal stresses during heating and cooling processes [5–7].

The most widely used method of depositing ceramic coatings upon developed metal surfaces is APS (Air Plasma Spraying) of LPPS (Low Pressure Plasma Spraying) together with EB PVD (Electron Beam Physical Vacuum Deposition). Coatings deposited by plasma spraying method feature significant relative volume of the pores, the presence of cracks with parallel and normal orientation to substrate as well as other defects which lower the adhesion and strengthen the coatings peeling and chipping off. The mentioned defects facilitate diffusion permeability of oxygen ions from gas medium through a coating and into a metal substrate or NiCrAlY bond coat where together with Cr and Al they form Cr_2O_3 and α-Al_2O_3 oxides upon the boundary of these materials. Thickness growth of these oxides during operations in high temperatures which are characterized by high *E* Young's modulus as well as varied specific volume in relation to ZrO_3–Y_2O_3 ceramic is the cause which generates acute structural stresses and cracks upon phases boundary [8–10]. This is the main mechanism which destroys coatings in the functioning as thermal barriers.

It is anticipated that laser melting which eliminates defects of coating structure deposited with plasma spraying method will improve their adhesion and durability. The aim of this paper is to define the laser melting conditions as well as determine the influence of this process upon the structure, selected physical properties and durability of ZrO_2–Y_2O_3 coatings functioning as thermal barriers.

2. Materials and methods

2.1. Choice of material for testing and samples preparation

Samples cut out of nickel base EI 868 super-alloy plate of 1.2 mm thickness containing ≤0.10 wt.%C; ≤1.0 wt.%Mn; ≤0.5 wt.%Si; 24–26 wt.%Cr; 0.3–0.7 wt.%Ti; ≤0.25 wt.%Al; 14–16 wt.%W; ≤0.10 wt.%Mn; 2.85 wt.%Fe [11] have been subjected to investigations. First, NiCrAlY (Amdry 961) alloy of 200 μm thickness and then another ceramic coating ZrO_2 + 8 wt.% Y_2O_3 (Metco 204B-NS) of 350 μm thickness and 8–16% porosity have been deposited by plasma spraying method upon their surface. Laser melting of ceramic coatings followed right through or at a depth of 200 μm. Chemical composition of powder mixtures Amdry 961 and Metco 204B-NS used for plasma spraying has been presented in Table 1.

Super-alloy samples of dimensions altered in order to meet the requirements of specific tests have been subjected to a flux of quartz sand of 200–300 μm granularity under pressure of 0.25 MPa prior to plasma spraying. Surface roughness of samples after sanding was 9.2 ± 2.3 μm. Plasma spraying of NiCrAlY bond coat and ZrO_2–Y_2O_3 top coat has been performed by METCO M7B apparatus with 6.5 mm diameter nozzle and vertical angle of 10° where the following parameters were used: Ar + H_2 gas mixture, voltage U = 70 V, current intensity I = 600 A, intensity of flow H_2—0.52 m^3/h and Ar—1.62 m^3/h, intensity of flow Ar-powder carrier of 50 °C—1.80 m^3/h, nozzle diameter of a powder feeder—2 mm and sample transfer rate relative to the nozzle—0.03 m/s.

The anticipated porosity of the coatings has been obtained by altering the distance between nozzle and sprayed surface as well as sample transfer rate relative to the nozzle. In order determine some chosen physical properties, ZrO_2–Y_2O_3 and NiCrAlY coats of 500 and 1000 μm thickness have been deposited by plasma spraying method of these powders upon NaCl film sprayed initially upon smooth surface of EI 868 super-alloy substrate. These coatings have been separated from metal substrate by dissolving NaCl film in water.

Laser melting of coatings right through or at a defined depth has been done by HPDL Rofin Sinar DL 020 diode laser of 0.1–2.5 kW power. Continuous radiation of 808 ± 5 nm wave length, 82×10^{-3} m focal distance and $(1.8 \times 6.8) \times 10^{-3}$ m focal spot dimensions has been applied. Melting conditions have been determined upon previously prepared model dependence chosen in the paper [13], altering laser power from 300–900 W. Samples positioned upon cool substrate or steel block heated up to 700 °C to reduce thermal stresses have been shield and cooled during laser treatment by argon flux of 0.2×10^{-3} m^3/s intensity of flow coming out of the nozzle of 12×10^{-3} m diameter.

It has been found that ceramic coatings deposited directly upon sanded surface of EI 868 super-alloy show the tendency to peel and chip off during laser treatment. High porosity coatings deposited upon NiCrAlY bond coat behave in a similar way. However, right through laser melting of coatings often leads to a serious damage of bonds upon the boundary between ceramic material and NiCrAlY bond coat which occurs due to significant difference in surface tension of these materials. In such conditions the melted coating shows discontinuity and high surface roughness since the drops of solidified ceramics featuring weak substrate bonds are being arranged in the line following the moving laser beam.

2.2. Methodology of examinations

The structure and selected physical properties of ceramic coatings deposited by plasma spraying method and in laser melted state have been determined by the method of light microscopy, X-ray qualitative and quantitative structural analysis, microanalysis of chemical composition, measurements of hardness, density and thermal conductivity, structural stability as well as resistance to cyclic temperature changes.

Metallographic tests as well as measurements of ZrO_2–Y_2O_3, NiCrAlY coat and super-alloy metal substrate hardness have been performed on transverse cross-sections of metallographic specimens, perpendicular to their surface with a deposited coating. The observations of the structure and boundaries of each separate sample coating have been performed on etched and non-etched metallographic specimens with the use of MF2 and Axiowert 405 microscope. Vickers method at the load of 50 mN and MF2 microscope attachment has been used for micro-hardness measurements of these coatings.

Porosity of coatings has been determined with the use of VICOM SUPERVIST computer system for image processing coupled with MF2 microscope. The obtained data have been verified with the density of coatings separated from substrate determined by piknometric method and theoretical density of ceramic calculated while taking into account Y_2O_3 concentration, atomic weights to the volume of phases elementary cells and their volume fraction in coatings [3,14].

Phase X-ray analysis method with the application of Philips X' Pert diffractometer has been adopted for the analysis of phase composition of Metco 204–NS powder, coatings deposited by plasma spraying method and the same coatings after laser melting. Monochromatic radiation Cu$K\alpha_1$ with a wave length λ = 0.15420 nm and a graphite monochromator at the side of diffracted beam has been applied. Measurements have been carried out by step method (0.02°) in 2θ angle range from 20–90° (qualitative analysis) as well as in 2θ angle range from 27–33° (quantitative analysis). The calculation time in the first case was 4 s and in the second one 20 s.

Relative volume fraction of ZrO_2 phases with cubic and tetragonal lattice at c/a = 1.01 [14,15] as well as monoclinic phase in powder mixture Metco 204B-NS and in coatings have been determined by Toraya method [16] with the Split

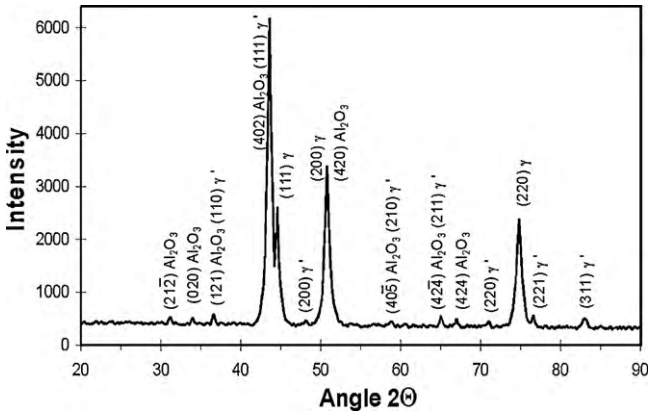

Fig. 1. XRD spectrum of bond coat NiCrAlY produced by APS method, obtained by the use of filtrated CuKα radiation.

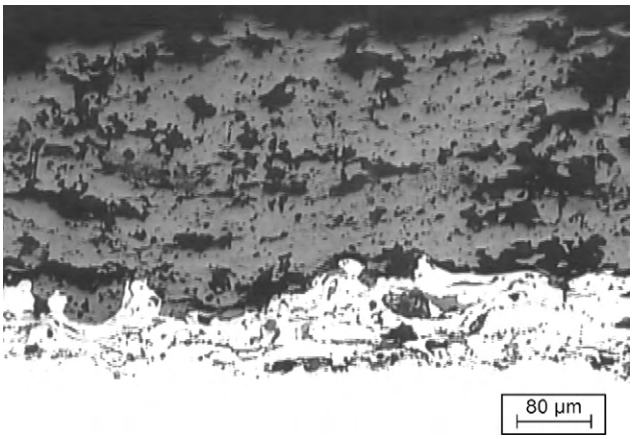

Fig. 2. Structure of ceramic coating with porosity 12.17% deposited by APS method upon NiCrAlY bond coat on the substrate of EI 868 alloy (not electrolytic etching).

Pearson VII asymmetric function for separating close or overlapping theoretical diffraction lines and PRO–FIT program for wave length $CuK\alpha_1 = 0.154059$ nm and $CuK\alpha_2 = 0.154439$ nm, according to the procedure quoted in papers [17,18]. Reliability coefficient for single theoretical diffraction lines which would correlate with those determined experimentally falls within the range from 5.2 to 3.3 which if compared with the data included in the paper [16] seems to be quite satisfactory.

The analysis of chemical composition of microareas of ceramic top coat and NiCrAlY bond coat has been carried out with the use of Joel X-ray microanalyser Superprobe 733. Both qualitative and quantitative microanalyses have been done by EDS method with Oxford Instruments Link 300 apparatus. However, in order to separate the series of overlapping peaks, Joel WDS spectrometer was applied. Relative error did not exceed 1%.

Measurements of thermal conductivity of EI868 super-alloy samples as well as those with deposited coatings by APS method have been done on the apparatus in the form of a column which enabled stable flow of heat flux [19].

Thermocouples positioned in the blocks which held the sample down enabled to determine temperature distribution, density of thermal fluxes penetrating the system as well as helped calculate thermal resistance values and thermal conductivity coefficients in the metal substrate of the samples and ceramic coatings featuring various porosities after plasma spraying and laser melting. The detailed procedure of determining thermal conductivity coefficients for homogeneous samples as well as those with deposited coatings has been given in the paper [13].

3. Examination results and discussion

3.1. The structure of EI 868 super-alloy, NiCrAlY bond coat and ceramic coatings deposited by plasma spraying and laser melting

EI 868 super-alloy of a chemical composition given in Table 1 features the structure of γ solid solution with f.c.c. lattice and small participation of γ′–Ni_3 (Al,Ti) phase with ordered $L1_2$ as well as $M_{23}C_6$ and M_6C carbides with regular complex lattices. The super-alloy after having been subjected to annealing in temperatures ranging from 1170 to 1200 °C and then to cooling in air, is used as creep-resisting one up to 800 °C, in which *E* modulus is 50 GPa, yield strength YS = 120 MPa, tensile strength UTS = 200 MPa, elongation *A* = 40%, reduction of area of specimen *Z* = 30% and creep strength $R_{z/100\,h}$ = 52 MPa. Once this temperature is exceeded, the properties such as strength and creep resistance of the alloy are lower.

NiCrAlY bond coat deposited by plasma spraying with Amdry 961 powder (Table 1) upon the surface of EI 868 super-alloy samples features multiphase structure on a base of γ solid solution with considerable participation of semi-coherent γ′ phase–Ni_3Al ($L1_2$) and oxides Al_2O_3 (Fig. 1). Heterogeneous chemical composition of this coating has been proved by EDS and WDS microanalyses in samples cross-sections and by analysis of isothermal cross-sections of NiCrAlY alloys phase equilibrium [20]. The absence of Al_2O_3 oxides in Amdry 961 powder mixture means that they are formed during plasma spraying process.

ZrO_2–Y_2O_3 ceramic coatings with 8–16% porosity deposited by plasma spraying upon NiCrAlY bond coat feature fine stratification and uniform distribution of pores provided the porosity is the lowest, due to the short distance between the nozzle of plasma gun and the sprayed surface. The increased porosity of coatings caused by longer distance between the nozzle and the sprayed surface results in their lower quality due to lower plasma temperature and higher viscosity of ceramic drops. Then large pores with developed form as well as cracks normal to the direction of plasma spraying emerge in coatings and also at the boundary ceramic coating–NiCrAlY bond coat (Fig. 2).

Laser melting process greatly affects the structure and hardness of ceramic coatings. Pores, microcracks and other defects developed during plasma spraying process disappear. However, laser melting of these coatings all through their thickness generates cracks and stratifications at the boundary ceramic coating–NiCrAlY bond coat (Fig. 3).

It is so since thermal tensile stresses are generated in coatings during the cooling process. This is due to lower thermal expansion of ceramic material and metal substrate. Only coatings partially laser melted preserve perfect bond between substrate and sample and show compact structure. It is true specially for coatings with low porosity, laser melted at samples preheated to the temperature of 700 °C (Fig. 4).

This does not ensure good quality of coatings which feature high relative volume of defects after plasma spraying. Although the melted area of coatings, similarly to the previously mentioned case, features compact structure and smooth surface both parallel and vertical local cracks occur (Fig. 5).

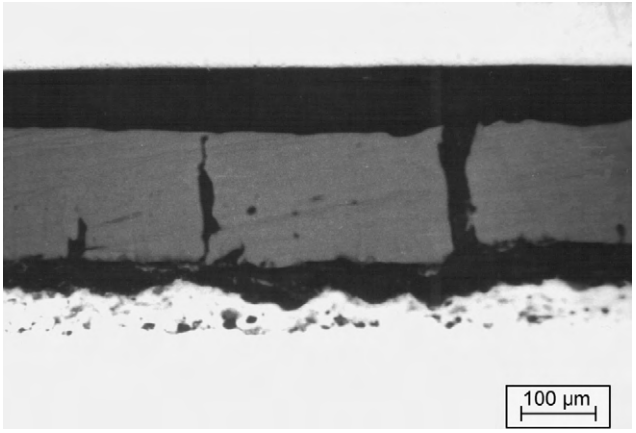

Fig. 3. Structure of ceramic coating ZrO_2–Y_2O_3 with porosity 15.23% fully laser melted; laser power 700 W, scanning rate 0.0125 m/s.

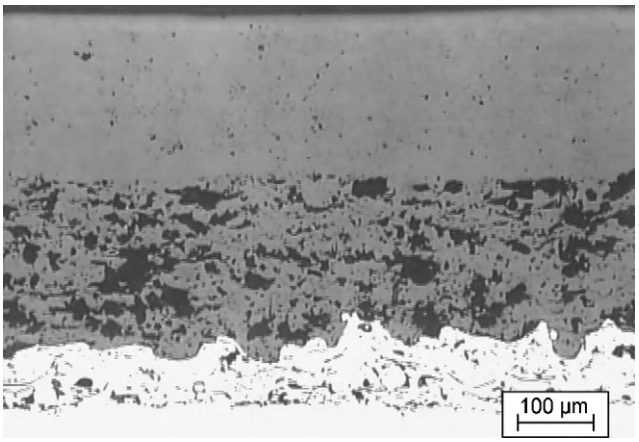

Fig. 4. Structure of ceramic coating ZrO_2–Y_2O_3 with porosity 7.46% partially laser melted; laser power 600 W, scanning rate 0.0083 m/s.

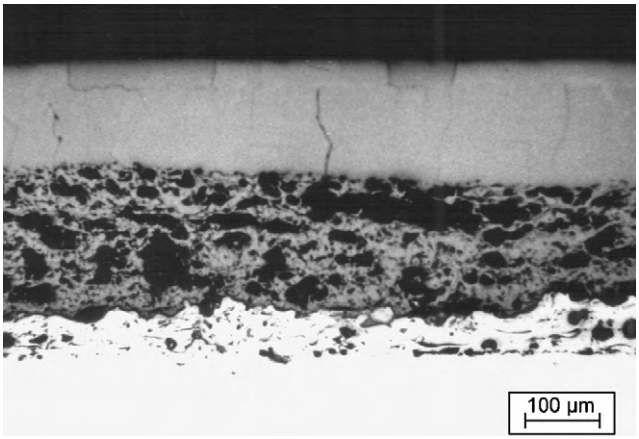

Fig. 5. Structure of ceramic coating ZrO_2–Y_2O_3 with porosity 15.23% partially laser melted on part of the thickness laser power 600 W, scanning rate 0.0083 m/s.

The fact that the number of pores and other structural defects developed during plasma spraying disappear, is the factor which decides that the hardness of laser melted coatings is much higher than those which were not subjected to such treatment. For example, the hardness of a coating with 7.46% porosity ranges from 1000 to 1200 $HV_{0.5}$ and increases after laser melting to about 1600 $HV_{0.5}$ (Fig. 6). Hardness of NiCrAlY bond coat is about 420 $HV_{0.5}$ while EI 868 super-alloy substrate is about 200 $HV_{0.5}$.

Laser melting significantly affects the phase composition of coatings in comparison with those plasma sprayed. It also affects

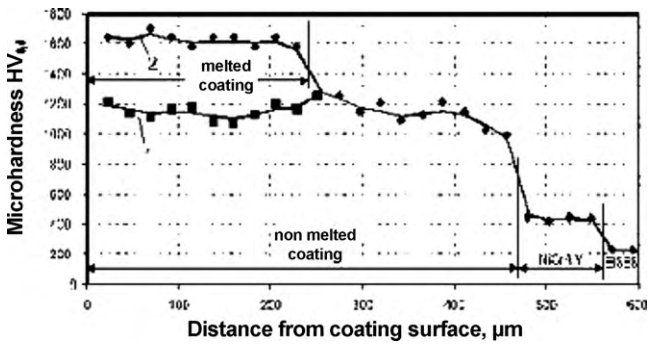

Fig. 6. Micro-hardness distribution on cross-section specimen including ceramic coating of porosity 7.46%, NiCrAlY bond coat and EI 868 alloy substrate; 1: plasma sprayed ceramic coating, 2: laser melted on part of the ceramic top coat thickness.

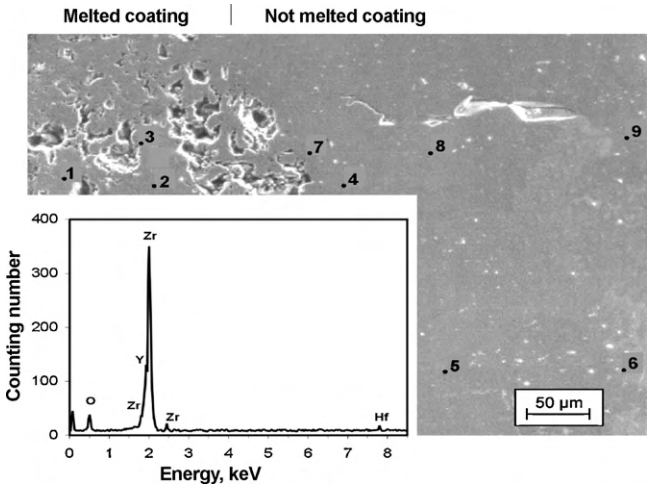

Fig. 7. View of cross-section ZrO_2–Y_2O_3 top coat: (a) not laser melted and melted (right), (b) spectrum of dispersed X-ray energy (EDS) in marked measuring points.

Metco 204B-NS powder mixture used for their production. The mixture contains all three allotropic forms of ZrO_2, i.e. with cubic, tetragonal and monoclinic lattice as well as slight participation of Y_2O_3.

ZrO_2–Y_2O_3 tetragonal phase has *c*/*a* lattice parameters nearly close to unity therefore the diffraction lines from lattice plane of cubic phase overlap with reflexes coming from defined lattice planes of tetragonal phase. ZrO_2–Y_2O_3 ceramic coating laser plasma sprayed features similar phase composition at lower intensity of diffraction lines from Y_2O_3 phase. It means that powder particles Y_2O_3 did not totally dissolve in ZrO_2 during plasma spraying. Thus ZrO_2–Y_2O_3 coatings deposited by this method feature heterogeneous chemical composition (Fig. 7 and Table 2).

Laser melting practically eliminates reflexes coming from lattice planes of Y_2O_3 and ZrO_2–Y_2O_3 phase with monoclinic lattices and differences in the intensity of diffraction lines from the same phases as shown in Fig. 8 result from recrystallization texture [13] generated in laser treated coatings.

The absence of diffraction lines from phases with monoclinic lattice in X–ray spectrum indicates homogenization of chemical composition of coatings arise during laser melting process. The data have been proved by X-ray microanalysis and WDS spectrometer [13].

Varied volume participation of ZrO_2–Y_2O_3 phase with monoclinic lattice in plasma sprayed and laser melted coatings has been also proved by Toraya method. The paper [13] states that volume participation of this phase in Metco 204B-NS powder mixture is 6.7% and decreases to 5.2% in coatings deposited by plasma spraying method and to 1.7% after laser melting. It means that during plasma spraying process, powder grains are transferred into doughy state

Table 2
Results of microanalysis (EDS) for ZrO_2–Y_2O_3 top coat in melted zone (points 1, 2, 3) and not melted zone.

Measuring points	Components (wt.%)			
	O	Zr	Y	Sum
1	23.90	69.74	6.35	99.99
2	25.18	68.92	5.89	99.99
3	26.62	67.11	5.27	99.00
4	23.77	69.76	6.44	99.97
5	23.20	70.20	6.70	100.10
6	22.68	70.23	7.02	99.93
7	24.14	69.18	6.67	99.99
8	22.78	71.23	5.98	99.99
9	22.55	70.05	7.07	99.67

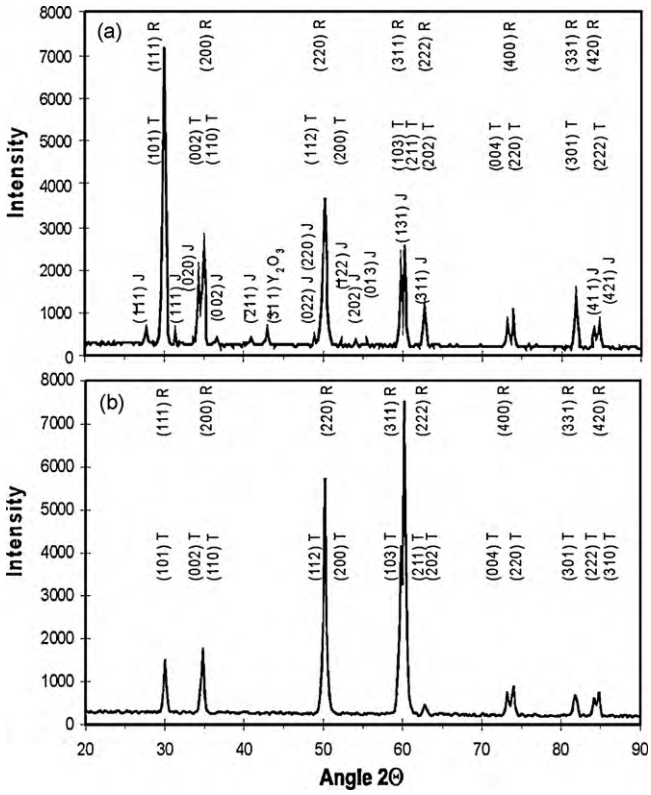

Fig. 8. XRD spectrum: (a) top coat ZrO_2–Y_2O_3 obtained by plasma spraying method, (b) top coat ZrO_2–Y_2O_3 after laser treatment; MTR – ZrO_2–Y_2O_3 phases properly with monoclinic, tetragonal and cubic lattices.

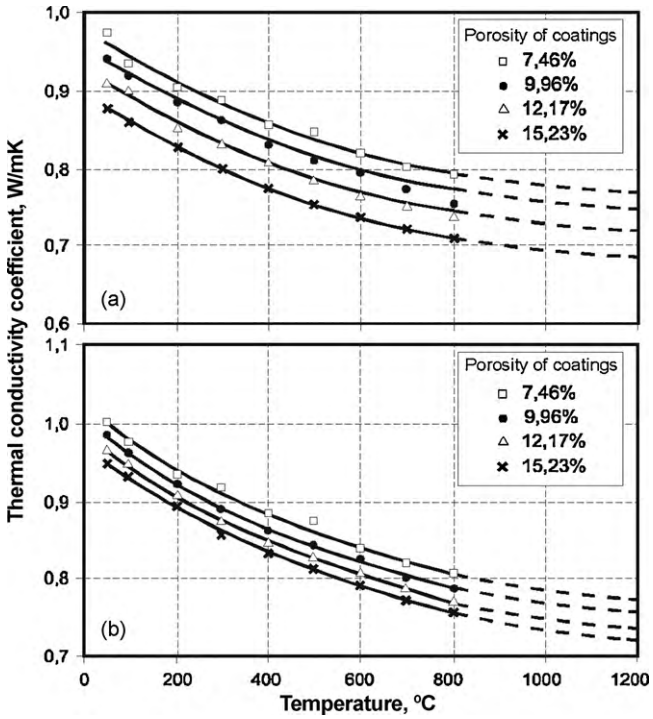

Fig. 10. Temperature dependence of thermal conductivity coefficient: (a) in ceramic coatings featuring various porosity obtained by plasma spraying method, (b) in ceramic coatings featuring various porosity laser melted on part of their thickness.

or their outer area is pitted without any possibility of diffusion homogenization of chemical composition of coatings. Due to the fact that HPDL laser with rectangular cross-section of beam has been used for laser melting, the roughness of coatings surfaces has been reduced in comparison with those deposited by plasma spraying. Their higher erosion resistance has been observed [13].

3.2. Structural stability and physical properties of ZrO_2–Y_2O_3 as thermal barriers

Dilatometric tests proved that EI 868 super-alloy features near linear dependence of relative elongation from temperature level of about 900 °C. Once the temperature is exceeded the linear dependence of relative elongation changes into parabolic one (Fig. 9).

It is closely connected with $M_{23}C_6$ carbides and γ′-Ni_3(AI,Ti) phase dissolution in γ a stable solution. Similar course of dilatometric curves is characteristic for the samples of this alloy with deposited plasma sprayed coatings ZrO_2–Y_2O_3 as well as after laser melting when tested in packs. Lower thermal extension of ceramic material in relation to the metal substrate reduces the gain in relative elongation of samples in the temperature function. The effect of relative elongation in temperature close to 900 °C is changing as well. It is caused by transformation of ZrO_2–Y_2O_3 with monoclinic lattice into tetragonal form which is accompanied by the change of relative volume of ceramic material by about 8%. The effect is initiated both at the heating and the cooling of samples with coatings deposited by plasma spraying method. It is the result of more active participation of ZrO_2–Y_2O_3 phase with monoclinic lattice in the coatings in comparison with those subjected to laser melting.

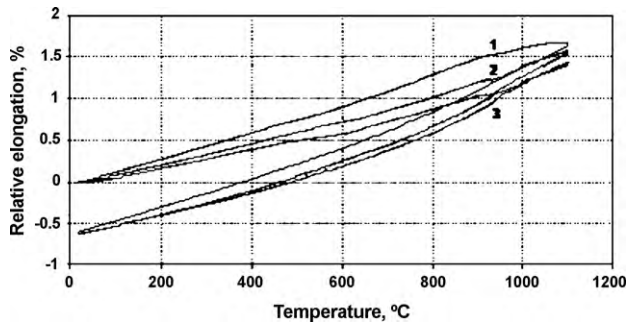

Fig. 9. Unit elongation in the direction of thickness of specimens in the function of heating and cooling temperature: 1: EI 868 alloy, 2: EI 868 alloy with obtained, plasma spraying top coat ZrO_2–Y_2O_3, 3: EI 868 alloy with laser melting ZrO_2–Y_2O_3, top coat.

Thermal conductivity in coatings. Temperatures of thermal fluxes penetrating the samples have been determined on the basis of test measurements. They helped calculate the values of thermal resistance of samples. When contact resistance value between blocks of measuring apparatus and samples surface has been determined experimentally it then enabled to find the thermal conductivity coefficient of ceramic coatings with varied thickness and porosity as well as in the laser melted state. The calculations have been done on the basis of measurements carried out in temperature range up to 800 °C. The thermal conductivity coefficient on the other hand in temperature above 800 °C was calculated according to the data included in the paper [19].

The measurements and calculations performed helped determine the temperature dependence of thermal conductivity coefficients of coatings with varied porosity (Fig. 10a) as well as after laser melting on part of the thickness (Fig. 10b).

The diagrams show that the thermal conductivity of the investigated coatings which have been deposited by plasma spraying method as well as after laser melting decreases when the testing temperature and porosity grow.

It was also found out that the temperature gradient over the coating thickness depends on the density of the heat flux pass-

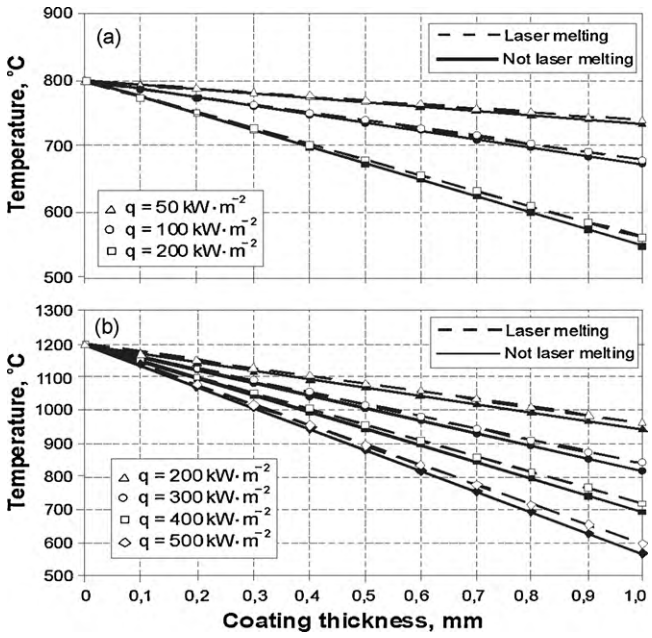

Fig. 11. Influence of heat flux density upon temperature distribution in ceramic coatings developed by plasma spraying method and laser treatment in depending on their thickness: (a) agent temperature from the side of ceramic coating equal 800 °C, (b) agent temperature from the side of ceramic coating equal 1200 °C; q: heat flux density.

ing through the sample, difference of temperatures of the opposite coating surfaces, and its state. The temperature gradient over the coating thickness with the particular porosity after the plasma spraying grows along with the heat flux density increase and with the increase of the difference of temperatures of the opposite surfaces of the sample [13]. Laser melting to about the half of the coating thickness results in the slight decrease of the temperature gradient (Fig. 11).

Calculations performed for a model sample helped discover the effect of temperature reduction in each separate zone of a specimen (Fig. 12) under the following conditions: stable heat flux with deposited ceramic coatings with 7.46% porosity and 1 mm thickness and laser melting into the depth of 0.3 mm, NiCrAlY coats with 250 μm and EI 868 alloy substrate of 1.27 mm thickness, coating surface temperature 1200, 1000, 800 and 20 °C on the other side of the sample. The diagram shows that the temperature in ceramic coating drops significantly together with its growth on the surface. The change in the coatings surface temperature from 1200 to

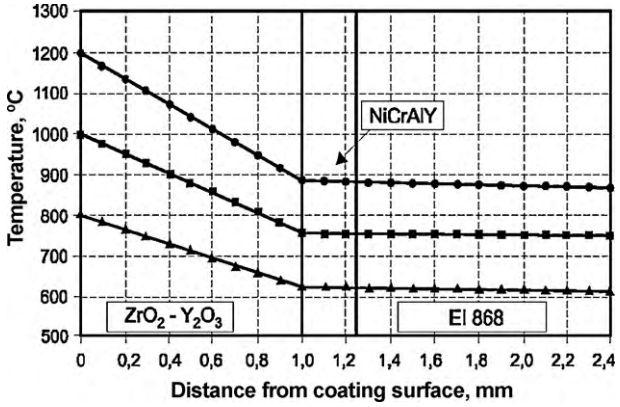

Fig. 12. Temperature distribution in ZrO_2–Y_2O_3 top coat–1 mm thick, in NiCrAlY bond coat – 250 μm thick and in metal substrate of specimen, under the steady heat flow conditions.

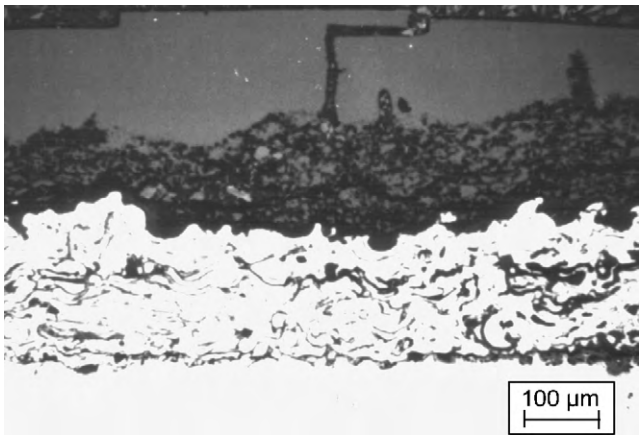

Fig. 13. ZrO_2–Y_2O_3/NiCrAlY coating laser melted through 60% of the thickness with laser power 600 W and scanning rate 0.0083 m/s, after 425 thermal cycles.

1000 and to 800 °C lowers the temperature on the coating featured by the mentioned thickness by 315, 240 and 188 °C, respectively. However, the decrease of temperature in metallic areas of samples in such circumstances is slight and equals 23, 20 and 18 °C, respectively. The effect of temperature fall in the coating with the same porosity and thickness, which has not been subjected to laser melting is slightly bigger and reaches the value of 322, 250 and 195 °C, respectively for temperatures of coating surface 1200, 1000 and 800 °C.

Thermal life prediction of ZrO_2–Y_2O_3 coatings. The investigations of the influence of thermal cycles, i.e. heating and holding of samples at1100 °C for 0.25 h and cooling in air to room temperature help discover that thermal life prediction the ZrO_2–Y_2O_3 top coat depends on their porosity after plasma spraying as well as on the laser melting conditions. Surface damages, cracks and chippings on the boundary with NiCrAlY bond coat after max tested number of 425 thermal cycles have not been detected only in case of coatings with low porosity of 7.46% deposited by plasma spraying and laser melting through about 50% of thickness upon samples preheated to about 700 °C. Slight damages in the form of surface microcracks lattice have been found in coatings on cool substrate subjected to laser melting (Fig. 13).

However, in case of coatings with more extensive porosity deposited by plasma spraying and then laser melted at varied depths, stratifications on the boundary with NiCrAlY bond coat as well as cracks perpendicular to their surface occur during cyclic temperature changes. This is all accounted for by thermal stresses which become active here. This also leads to chipping and peeling off which is initiated in the corners and along the edges of the sample (Fig. 14).

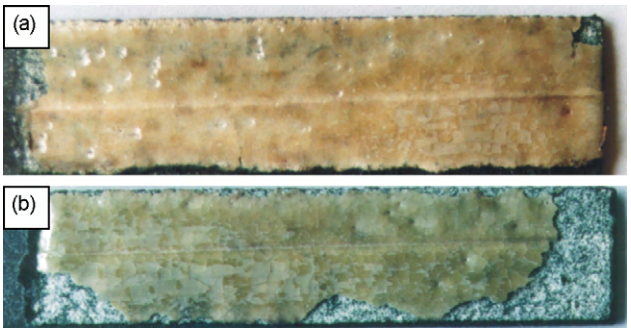

Fig. 14. View of laser melted surface coating ZrO_2–Y_2O_3 all through its thickness: (a) After 295 thermal cycles, (b) after 425 thermal cycles.

4. Conclusions

The performed investigations proved that the transfer of ceramic material into liquid state during laser melting: reduce pores and other structural defects which occur in coatings during plasma spraying process, improves homogeneity of chemical composition and diminishes phase ZrO_2–Y_2O_3 with monoclinic lattice participation and lowers structural stresses connected with transformation of this phase during heating and cooling. Moreover, tightness, hardness and erosion resistance of the coatings are higher.

Elimination of structural defects of coatings during laser melting improves thermal conductivity of the ceramic material and lowers the temperature gradient on coatings thickness, which strongly depends on their porosity after plasma spraying, and in case of melting performed all through the thickness weakens their adhesion to metal substrate due to low wettability of metals by ceramic material and forming of cracks and stratifications upon boundary of these material.

Coatings featuring low porosity after plasma spraying, laser melted on part of their thickness carried out upon heated up to about 700 °C metal elements seem to posses the highest thermal life prediction in the conditions of cyclic temperature changes from 20 to 1200 °C. This fact causes the reduction of structural stresses on the boundary with metal substrate and connected with the change of volume of ceramic material during crystallization. Besides thermal stresses resulting from varied thermal expansion of these materials are reduced as well.

Coatings featuring low porosity and laser melted on part of their thickness when compared with those deposited by plasma spraying method demonstrate slightly better thermal conductivity and smaller temperature gradient on the thickness which depends on thermodynamic factor temperature upon the coating surface as well as on the density of heat flux. These coatings preserve abovementioned physical properties also in conditions of steady heat flow. As far as thermal life prediction is concerned in the conditions of cyclic temperature changes these coatings meet all requirements of thermal barriers.

References

[1] M.J. Stiger, N.M. Yanar, Zeitschrift fur Metallkunde 90 (1999) 1069–1078.
[2] R. Wing, Materials World 8 (3) (2000) 10.
[3] T. Sakuma, Transactions of the Japan Institute of Metals 29 (11) (1988) 879–893.
[4] M. Belmonte, Advanced Engineering Materials 8 (8) (2006) 603–703.
[5] H.B. Guo, R. Vassen, D. Stover, Surface and Coatings Technology 192 (2005) 48–56.
[6] G. Bertrand, P. Bertrand, P. Roy, C. Rio, R. Mevrel, Surface and Coatings Technology 202 (2008) 1994–2001.
[7] V. Teixeira, M. Andritschky, H. Gruhm, W. Mallner, H. Buchkremer, D. Stover, in: C. Berndt (Ed.), Proceedings of the 8th National Thermal Spray Conference, ASM International, Houston, USA, 1995, pp. 515–520.
[8] J.A. Haynes, M.K. Ferber, W.D. Porter, E. Rigney, Oxidation of Metals 52 (1/2) (1999) 31–76.
[9] V. Teixeira, M. Andritschky, W. Fischer, H. Buchkremer, D. Stover, in: T. Ericson Linköping (Ed.), Proceedings of the 5th International Conference Residual Stresses–ICRS'5, Sweden, June, vol. I, 1997, p. 436.
[10] V. Teixeira, M. Andritschky, W. Fischer, H. Buchkremer, D. Stover, Surface and Coatings Technology 120–121 (1999) 103–111.
[11] Load capacity of gas turbine blades under the influence of non-stationary thermal and loading field, Ukrainian Academy of Science–Soviet Union, Institute of Strength Problems at Naukovaja Dumka Kiev (1975), pp. 146–153.
[12] Sulzer – Metco the Coatings Company, Materials Guide, Revised December (1999).
[13] K. Kobylańska-Szkaradek, Zeszyty Naukowe Politechniki Śląskiej–Mechanika (in polish) (Scientific Journal of Silesian University of Technology–Mechanics), nr 154, Gliwice (2005).
[14] J.P. Brandon, R. Taylor, Surface and Coating Technology 39/40 (1989) 143–151.
[15] R. Taylor, J.P. Brandon, P. Morrell, Surface and Coating Technology 50 (1992) 141–149.
[16] H.J. Toraya, Journal of Applied Crystallography 19 (1986) 440–447.
[17] H.J. Toraya, M. Yoshimura, S. Somiya, Communications of the American Ceramic Society June (1984), pp. C 119–121.
[18] R.A. Miller, J.L. Smiałek, G.G. Garlick, in: A.L. Heuer, L.W. Hobbs (Eds.), Advances in Ceramics, vol. 3, The American Ceramics Society, Columbus/Westervillem, OH, USA, 1981, pp. 241–253.
[19] K. Kobylańska-Szkaradek, Inżynieria Materiałowa (in polish) (Material Engineering) 3 (140) (2004) 604–606.
[20] R. Decker, Climax Molibdenum Company Symposium Zurich (1969) 17–20.